Eidgenössische Technische Hochschule Zürich
Swiss Federal Institute of Technology Zurich

Quantum Device Lab

Semester Thesis

Metastable Helium source

by Lukas Gerster

Supervisor:
Tobias Thiele

Principal Investigator:
Prof. Dr. Andreas Wallraff

July 12, 2014

Abstract

In this thesis, a source of metastable $3S_1$ Helium atoms (He^*) is characterized. Using two skimmers, an angle of divergence of $\approx 1^o$ can be achieved. Further the use of laser cooling for improved collimation is prepared and outlined.

Contents

1 Theory

The theory section about the behaviour of molecular beams is mostly based on [1], the section about laser cooling is based on [2].

Metastable Helium states are the typical starting state for producing Rydberg atoms with laser excitations. The long lifetime [3] $\tau \approx 7900s$ of the metastable $1s^1 2s^1\ {}^3S_1$ triplet state of helium results from the fact that spontaneous emission to the ground state $1s^2\ {}^1S_0$ is optically forbidden due to the selection rules on l and s. For the purpose of the experiment, the lifetime is much longer than the duration of the measurement, and spontaneous decay can be neglected.

1.1 Beam expansion

In this section the production of a molecular beam is presented. The setup consists of a gas reservoir at constant pressure p_0 and a large chamber at ambient pressure p_b. The gas in the reservoir is at temperature T_0, and can stream into the chamber through an orifice of size d.
For a gas passing through the orifice there are two distinct regimes, the effusive regime and the supersonic regime. Whether the expansion is supersonic or not is dependent on the mean free path λ_0 of the atoms at the nozzle, for $\lambda_0 \gg d$ the beam is effusive, and for $\lambda_0 \ll d$ the beam is supersonic.

Mean free path The mean free path λ_0 is the average distance travelled by a particle between two collisions. Therefore it can be written as

$$\lambda_0 = \frac{\bar{v}}{f}, \tag{1.1.1}$$

where $\bar{v}$ is the average velocity and f is the collision frequency. The collision frequency is given by

$$f = \sqrt{2} n \pi a^2 \bar{v}, \tag{1.1.2}$$

where a is the diameter of a particle and n is the particle density, which is given by the ideal gas law.

$$n = \frac{p_0}{k_B T_0}. \tag{1.1.3}$$

Put together one gets the expression

$$\lambda_0 = \frac{k_B T_0}{\sqrt{2} p_0 \pi a^2} \tag{1.1.4}$$

for the mean free path.

Effusive beams For a free path length much larger than the size of the orifice, particles escape from the reservoir without colliding with each other. Thus the velocity distribution and all distributions over internal degrees of freedom do not change, and remain the same as inside the reservoir; i.e. there is no thermalization.
The velocity inside the reservoir and in the beam is given by the Maxwell-Boltzmann distribution

$$P_M(v) \propto v^2 \exp\left(-\frac{mv^2}{2k_BT}\right), \tag{1.1.5}$$

Supersonic beams In the supersonic regime, the velocity of particles does not remain constant passing though the orifice. The particles undergo many collisions as they escape from the reservoir and thus thermalize. This causes an increase in velocity of the beam, which can be denoted by the Mach number $M = \frac{\bar{v}}{c}$, where c is the speed of sound in the medium. For an ideal gas, this speed is given by

$$c = \sqrt{\frac{\gamma k_B T}{m}}. \tag{1.1.6}$$

The zone of silence (see Fig. 1.1) is the region in which the dynamics of the flow can be described linearly, while the outer region experiences non-linear flow dynamics. Thus the zone of silence is favourable to extract a molecular beam. It extends to

$$x_M = 0.67d\sqrt{\frac{p_0}{p_b}} \tag{1.1.7}$$

In our case we have a diameter $d = 0.5\ mm$, and the pressures $p_0 =$ 6bar, $p_b = 10^{-7}$mbar, which gives a value $x_m^{He} = 82\ m$.
In conclusion for a supersonic expansion the reservoir pressure should be as high as possible, p_b should be as small as possible, and the temperature T_0 should be as low as possible for an optimal supersonic beam expansion.

1.2 Laser cooling

To reduce the transverse velocity of the beam of metastable helium, a series of skimmers is first employed to select only atoms with low initial transverse velocity. Further reduction of the transverse velocity is possible by means of laser cooling. In the following section the mathematical description of a laser cooling setup is derived. Laser cooling was first suggested independently by

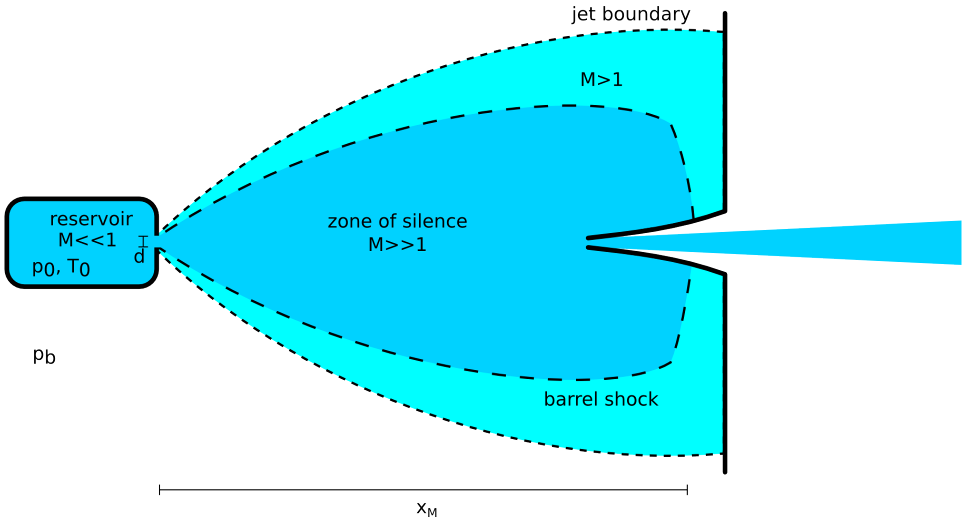

Figure 1.1: Drawing of a supersonic beam expanding from a reservoir into a chamber.The skimmer is placed to extract the beam from the zone of silence, and avoid the turbulent zone between the barrel shock and the jet boundary.

David Wineland and Hans Dehmelt in 1975, and later successfully demonstrated by Wineland, Drullinger, and Walls in 1978 [4]. The technique is based on the phenomena of light pressure, the fact that photons not only carry energy but also momentum. A photon carries momentum $\hbar k$ which is transferred to the atom when the photon gets absorbed. The atom is now in an excited state, and either spontaneously decays, or re emits the photon due to stimulated emission. In the second case, no net momentum transfer occurs, as the photon is emitted in the same direction as the absorbed one. In the first case however the direction in which the photon is emitted is random. For many events this leads to a total momentum transfer of

$$\Delta\vec{p} = \sum_N \hbar\vec{k} - \sum_N \hbar\vec{k'} = N\hbar\vec{k}, \tag{1.2.1}$$

as the momentum of spontaneously emitted photons averages out to 0.
The force acting on a single atom is then given by

$$\vec{F} = \frac{\Delta\vec{p}}{\Delta t} = \langle\frac{dN}{dt}\rangle\hbar\vec{k}. \tag{1.2.2}$$

To determine the rate $\langle \frac{dN}{dt} \rangle$ one has to consider the optical Bloch equations [5]. For a two level system one can write the density matrix as

$$\rho = \begin{pmatrix} \rho_{ee} & \rho_{eg} \\ \rho_{ge} & \rho_{gg} \end{pmatrix} = \begin{pmatrix} c_e c_e^* & c_e c_g^* \\ c_g c_e^* & c_g c_g^* \end{pmatrix}. \tag{1.2.3}$$

The time evolution is given by the equation

$$i\hbar \frac{d\rho}{dt} = [\hat{H}, \rho]. \tag{1.2.4}$$

One assumes $\hat{H} = \hat{H}_0 + \hat{H}_1$, where the two states are eigenstates of $\hat{H}_0$, and one defines $\hbar\Omega = \langle e|\hat{H}_1|g\rangle$. With $\Gamma = \frac{1}{\tau}$, where τ is the lifetime of the excited state one gets the following set of equations:

$$\frac{d\rho_{gg}}{dt} = \Gamma\rho_{ee} + \frac{i}{2}(\Omega^*\tilde{\rho}_{eg} - \Omega\tilde{\rho}_{ge}), \tag{1.2.5a}$$

$$\frac{d\rho_{ee}}{dt} = -\Gamma\rho_{ee} + \frac{i}{2}(\Omega\tilde{\rho}_{ge} - \Omega^*\tilde{\rho}_{eg}), \tag{1.2.5b}$$

$$\frac{d\tilde{\rho}_{ge}}{dt} = -(\Gamma/2 + i\delta)\tilde{\rho}_{ge} + i\frac{\Omega^*}{2}(\rho_{ee} - \rho_{gg}), \tag{1.2.5c}$$

$$\frac{d\tilde{\rho}_{eg}}{dt} = -(\Gamma/2 - i\delta)\tilde{\rho}_{eg} + i\frac{\Omega}{2}(\rho_{gg} - \rho_{ee}), \tag{1.2.5d}$$

where $\tilde{\rho} = \rho\exp(-i\delta t)$ and $\delta = \omega - \omega_0$ is the detuning. As the system is closed, $\rho_{gg} + \rho_{ee} = 1$, and due to optical coherence $\rho_{eg} = \rho_{ge}^*$. We are only interested in the steady state solutions of these equations, and introduce the population difference $w = \rho_{gg} - \rho_{ee}$. The derivatives $\dot{w}$ and $\dot{\rho_{eg}}$ vanish by assumption. This leads to the equations

$$0 = \frac{dw}{dt} = \Gamma(1 - w) - i(\frac{\Omega}{2}\rho_{eg}^* - \frac{\Omega^*}{2}\rho_{eg}) \tag{1.2.6a}$$

$$0 = \frac{d\rho_{eg}}{dt} = -(\Gamma/2 - i\delta)\tilde{\rho}_{eg} + i\frac{\Omega w}{2}. \tag{1.2.6b}$$

In the steady state, the number of absorbed and emitted photons are equal, therefore $\langle \frac{dN}{dt} \rangle = \rho_{ee}\Gamma$. These equations can be solved and plugged into Eq. 1.2.2, and one obtains

$$\vec{F}(\delta) = \hbar\vec{k}\frac{\Gamma}{2}\frac{\Omega^2/2}{\delta^2 + \Gamma^2/4 + \Omega^2/2}. \tag{1.2.7}$$

The force can be increased by raising the intensity $I \propto \Omega^2$, which eventually saturates of the value

$$\vec{F} = \hbar\vec{k}\frac{\Gamma}{2}. \tag{1.2.8}$$

1.3 Optical Molasses

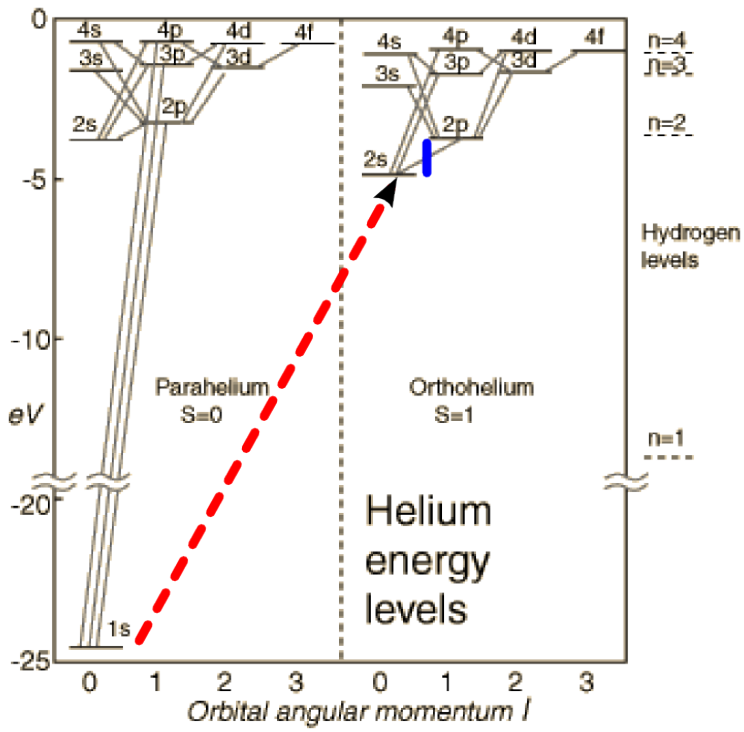

Figure 1.2: Energy levels of helium. Marked in red is the transition from He to He^*, as well as the cooling transition between 2^3S_1 and 2^3P_2 (blue). Image taken from [6]

In this experiment the cooling makes use of the $2^3S_1 - 2^3P_2$ transition. This transition is closed, meaning the 2^3P_2 can only decay back into the 2^3S_1, ensuring the metastable atoms are in an effective two-level system.
An atom with a finite velocity $v_a > 0$ experiences a Doppler shift, changing the resonance frequency of the transition ω_0 to $\omega_0 - \vec{k}\vec{v_a}$, and therefore shifts the detuning to $\delta' = \delta - \vec{k}\vec{v_a}$.
As a single beam can only apply force in one direction, a cooling scheme requires counter propagating beams. Restricted to one dimension the force can be written as

$$F(\delta - kv) - F(\delta + kv) \approx -2\frac{\partial F}{\partial \delta}kv := -\alpha v \tag{1.3.1}$$

This assumes that the forward and backward force are independent from each other, which is true as long as the system is far away from saturation.

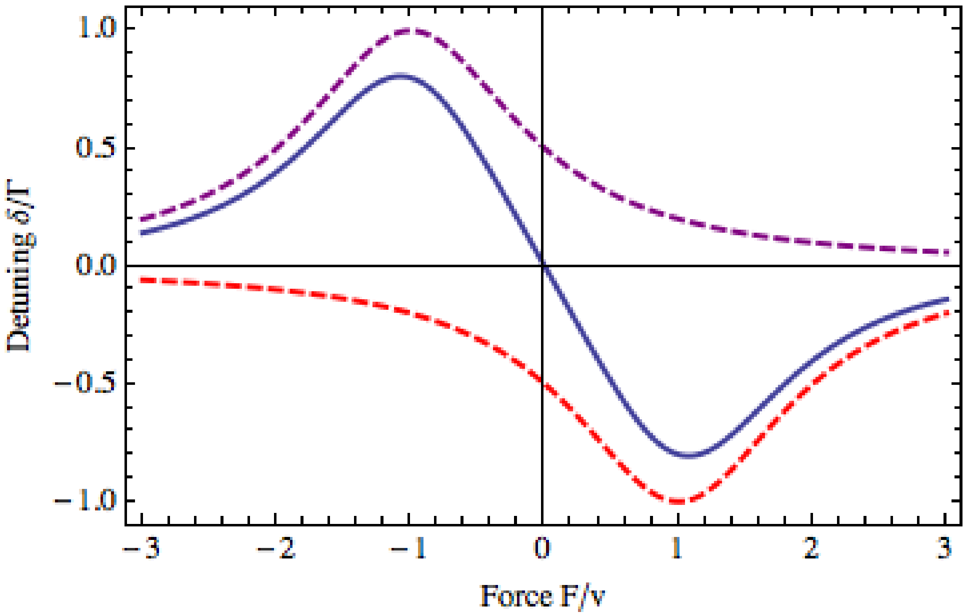

Figure 1.3: Force acting on an metastable atom due to two counter propagating beams as function of the detuning.

In this approximation the laser force always acts opposite to the velocity of the atom, slowing it down arbitrarily close to zero. However the momentum transfer is quantized and an individual photon imparts a momentum change of $\Delta\vec{p} = \hbar\vec{k}$. At this level fluctuations become important, and our approximation is no longer valid.
Before we reach that level, the assumption of two independent beams breaks down, as the natural linewidth γ has not been taken into account. Here the atoms can absorb photons from either beam, so no further cooling takes place. The limiting temperature is called the Doppler temperature $T_{Doppler}$, and is given by [5]

$$k_B T_{Doppler} = \frac{h\gamma}{2}. \tag{1.3.2}$$

In practice the laser is locked to the resonance frequency and the detuning is controlled by changing the angle between the laser beam and the beam of atoms 1.4, as the Doppler shift is dependant on the projection of the velocity of the atom onto the direction of the laser beam. The inclined

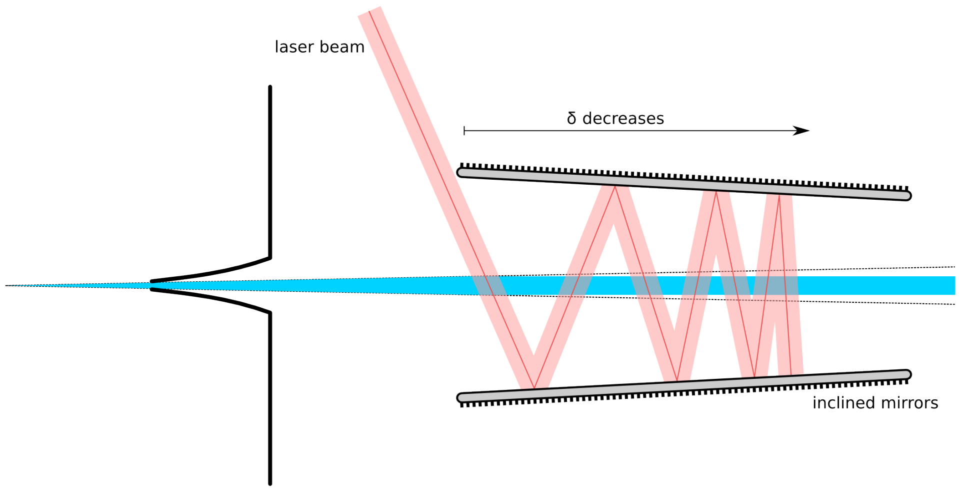

Figure 1.4: Alignment of laser beams for cooling metastable He^* atoms. The angles of the mirrors and beams are exaggerated.

mirrors reduce the angle between the laser beam and the perpendicular to the atomic beam, thus lowering the detuning.

1.4 Spectroscopy

Laser cooling requires laser beams whose frequency is accurately controlled. For the frequencies required the fluctuations are too large for manually tuning the system, thus requiring a feedback loop to stabilize the frequency.
This is done using a Doppler-free saturation spectroscopy cell [7]. In the cell metastable Helium atoms are generated. Absorption of photons by the metastable atoms leads to a decrease in the transmission spectrum at the particular transition frequency and forms a Lorentzian with a width of several Megahertz. Due to the temperature of the atoms the dip is Doppler broadened out into the Gigahertz range. This effect is much larger than the width of the transition, making it impossible to accurately determine the resonance frequency (Fig. 1.5a).

This can be solved by passing the vapour cell twice. A pump beam saturates the Helium atoms. Some light is reflected as probe beam. For exactly resonant light (only at zero longitudinal velocity) an atom can both be resonant with the pump and the probe beam. As the atoms are saturated by the pump beam, the photons from the probe cannot be absorbed, lead-

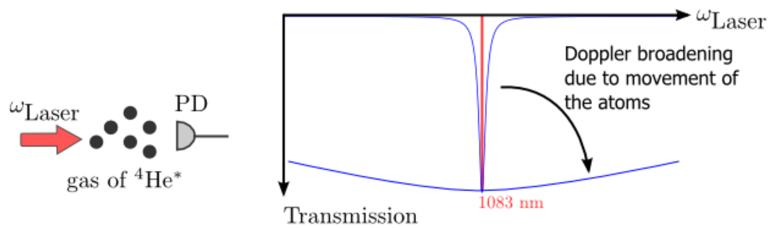

(a) The dip in the transmission spectrum is broadened out due to Doppler shift.

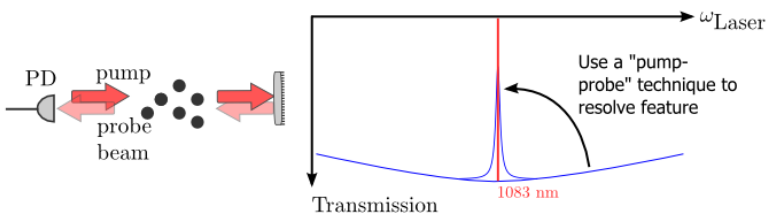

(b) By passing the beam twice through the spectroscopy cell, at the resonance frequency a Lamb dip appears.

Figure 1.5: Image taken for project documentation.

ing to an increase in the transmission spectrum (Fig. 1.5b). In this setup, a polarizing beam cube (PBS) only lets through vertically polarized light, which is turned to σ^+ polarized light by the $\lambda/4$ plate. At the mirror the polarization changes from σ^+ to σ^- polarized. The beam is then changed to horizontal polarization by passing a $\lambda/4$ plate again. The PBS then deflects the probe beam towards the detector. (Fig. 1.6).
The feedback loop to stabilize the laser needs an error signal. The absorption spectrum is however symmetric around the minimum, meaning it is impossible to find out if the wavelength is too short or too long if one tries to lock to the minimum. Locking to a set value is possible, however the signal is strongly dependent on the beam intensity. The Pound-Drever-Hall technique allows to generate an error signal that has a zero crossing. This allows easy locking of the laser to the resonance frequency, and is independent of the intensity of the beam. [8]

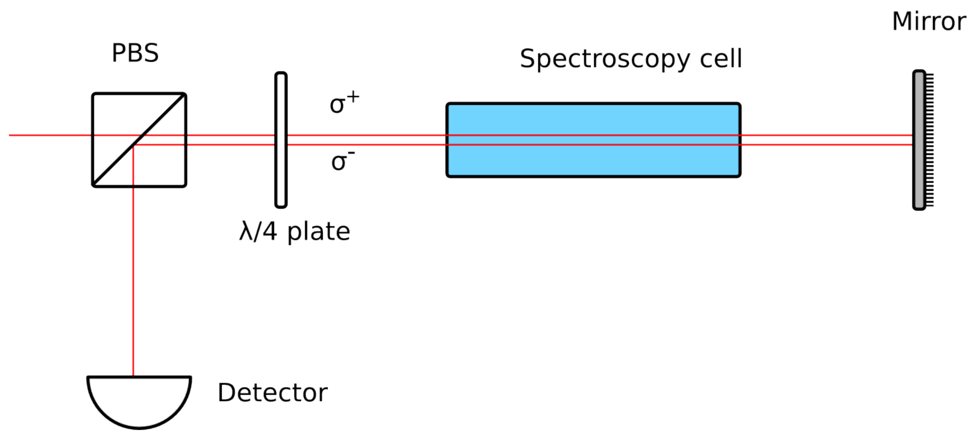

Figure 1.6: The beam passes the spectroscopy cell and is reflected at the mirror. The reflected probe beam is deflected at the PBS cube to the detector.

2 Experimental Setup

The setup 2.1 consists of three chambers, the source chamber, cooling chamber and the detection chamber. Two pumps are used to bring the chamber to a pressure of about 10^-7 mbar.

2.1 Source

The metastable helium atoms used in the experiment are generated in the source chamber. Continuous sources can be constructed using a discharge, applying a voltage of 300 V between a tip and the nozzle of the valve. Some helium atoms are ionized, and travel towards the tip, leading to a discharge, and this generates a current that flows between tip and nozzle. As the electrons hit He atoms, they knock out more electrons which are accelerated towards the nozzle, hitting other helium atoms. These electron impacts promote He to the metastable He^* state.
The source required for this experiment however has to operate in a pulsed mode at a frequency of $25Hz$. Compared to a continuous source the density inside the beam is higher by orders of magnitude. The discharge needs time to establish the current, as the helium gas is neutral, so charge carriers need time to build up first.
This problem is addressed by the addition of a filament heater (Fig. 2.2). A current of $\approx 5A$ flows through the filament, injecting electrons into the

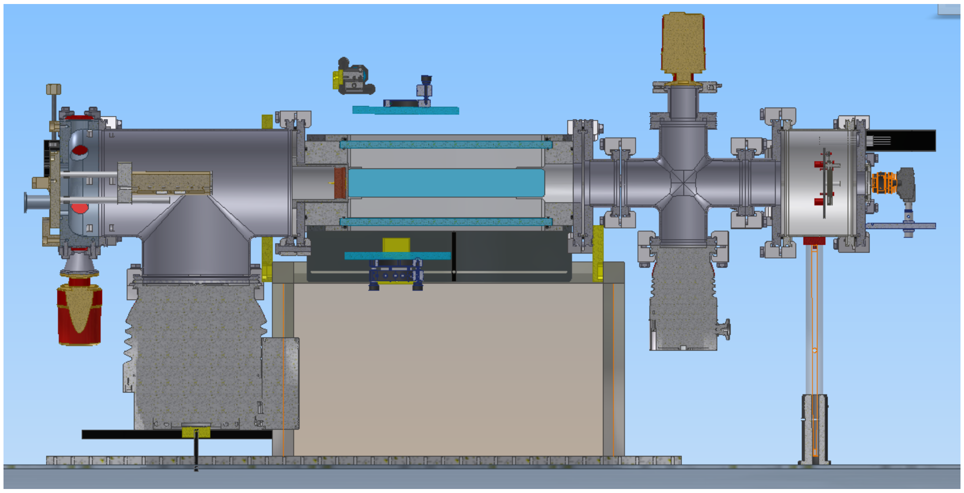

Figure 2.1: Experimental setup. Visible are source chamber, cooling chamber and the detection chamber. Image taken for project documentation.

discharge. The current is provided by a current source transforming 230V AC (Fig. C.1). A calibration measurement (Fig. 2.3) shows that the scale matches the actual output. The seeding of electrons as charge carriers leads to a faster build up of the discharge as it lowers the voltage required. In the experiment $280V$ were applied to the discharge tip. This allows the discharge to operate in a quasi-steady-state during the pulse. The addition of the electrons has the additional effect of enlarging the discharge region further out to areas of lower particle density, which increases the production of metastable atoms and reduces de-excitations of already produced metastable atoms to collisions [9].

2.2 Micro Channel Plate

A Micro Channel Plate (MCP) is used to detect the metastable atoms. The device consists of three plates; a front, back and a phosphor plate. The front and back plate contain a large number of tiny tubes with a diameter of $10\mu m$ each, every tube acting as an electron multiplier if a potential difference is applied between the front and the back plate of the MCP (Fig. 2.4). A single metastable atom hitting a tube knocks out a multitude of electrons, which are accelerated down the tube, knocking out more electrons as they hit the walls of the tube. Per initial impact about 10^7 electrons are produced.

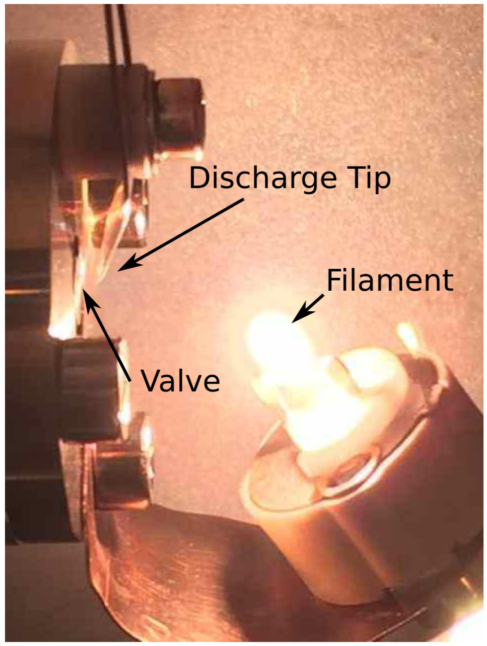

Figure 2.2: Source in operation. Visible are the valve, the discharge tip and the filament.

The electrons emerging from the plate are further accelerated towards the phosphor screen. The phosphor screen then provides spatial information about the incoming metastable atoms, while the drop in voltage between the plates provides temporal resolution.
The MCP is connected to the high voltage sources by a voltage divider. It splits the voltage applied to the back port at a ratio of approximately 1 : 5 between front plate and back plate (Fig. 2.5). The front port is used to directly apply a voltage to the front plate. The Phosphor screen has a separate port. The signal port can be used to read out the voltage drop between front and back gate when the beam hits the MCP, causing a current to flow between front and back plate.
In our experiment a voltage of $1.7kV$ was applied at the back port and a voltage of $4.5kV$ at the phosphor screen. At the front port an additional voltage of $500V$ is applied in pulsed mode. The MCP is only sensitive to events with this additional voltage, allowing to selectively detect metastable He atoms and filter out ions and photons that can also produce a signal, but arrive before the metastable atoms.
The circuit diagram for the voltage divider can be found in B. The full

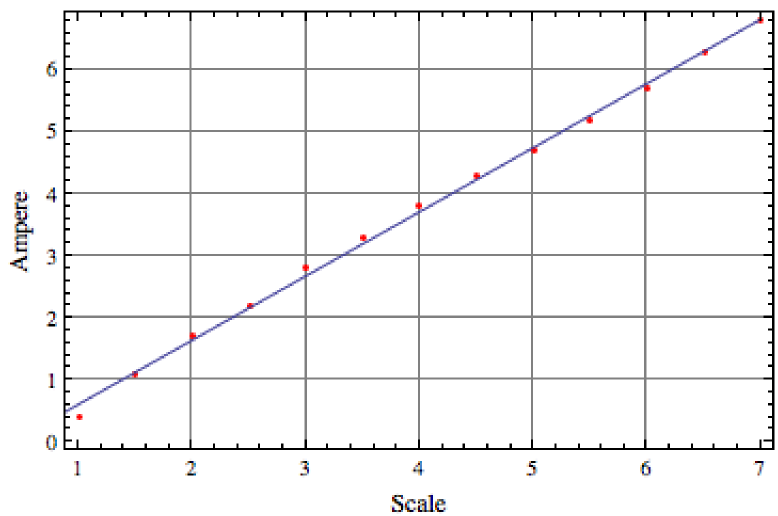

Figure 2.3: Calibration curve of the scale of the AC source.

control electronics can be found in [10].

2.3 Camera

A Thorlabs DCC1545M camera is mounted outside the beam chamber facing the phosphor screen of the MCP through a view port. The camera is connected by USB to the measurement computer.

The measurement software has two operating modes, video and capture (Fig. A.1). The video mode continually takes pictures and displays them to the user, while the capture mode takes a given number of pictures and averages the values. Captured pictures are saved both as raw data as well as .bmp image file. The software can be used without trigger, or taking an external trigger signal from the experiment via a USB data card. For the external trigger a delay can be set to offset the image capture. The trigger cycles option allows the program to only wait for the trigger after the given number of images were captured, as the recognition of the trigger has shown to be unreliable, leading to short wait times. The camera exposure time can be set.

The Labview software consists of a main loop and a control loop (Fig. A.2). After initialization the main loop runs continuously, requesting data from the camera as well as sending commands to it. All interfacing with the camera is done via the subVIs provided by the manufacturer Thorlabs. The two main modes video and capture are implemented with a case structure.

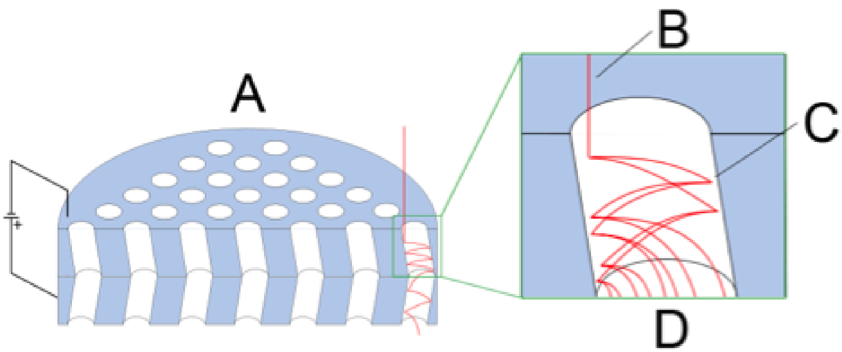

Figure 2.4: A:Tilted tubes in chevron arrangement. B:Incoming particle hits tube wall. C: Secondary hits by emitted electrons. D: Emitted electrons are accelerated towards phosphor screen. Image taken from [10]

In video mode the loop requests an image from the camera and displays it. No information is stored in this case. Capture mode takes a number of consecutive images and averages the result. If the save option is turned on, the image is numbered and saved, with a check to prevent overwriting of previous measurements.
The control loop monitors the user interface, and relays all changes to the main loop. This allows the interface to remain responsive even while the main loop is busy.
Aborting the program can leave Labview unable to reconnect to the camera, because the camera handle is not properly freed. In this case restarting Labview resolves the problem.
During the writing of this thesis, the program was modified slightly, e.q. it is now possible to subtract a captured picture as background.

2.4 Spectroscopy Setup

The laser for the Doppler free saturation spectroscopy setup emits linearly polarized light. Sidebands are modulated onto the beam for the Pound-Drever-Hall technique by means of fiber-based EOM. The polarization axis is controlled with a $\lambda/2$ plate. The beam passes the PBO cube and enters through a $\lambda/4$ plate the spectroscopy cell, a helium filled tube, where the atoms are excited to the metastable state using a coil.
The reflected beam is reflected out at the PBO cube, and is split up between

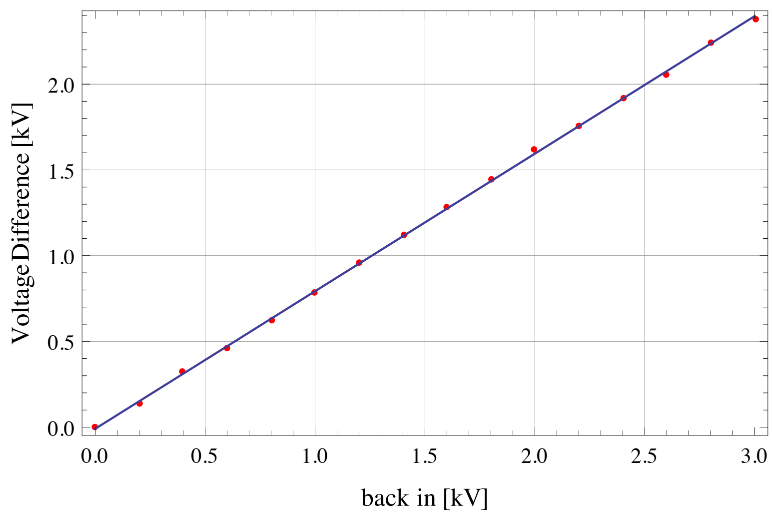

Figure 2.5: Voltage difference between front and back plate as function of applied voltage at the back port.

a photo diode, which measures the absolute intensity as well as a lock in setup, which generates the error signal to which the beam is locked to.
The metastable atoms are produced by applying a AC current through a coil around the spectroscopy cell. The cell has been rewired, and now reliably produces a discharge. Depending on the pressure in the cell different states are activated (Fig. 2.6).

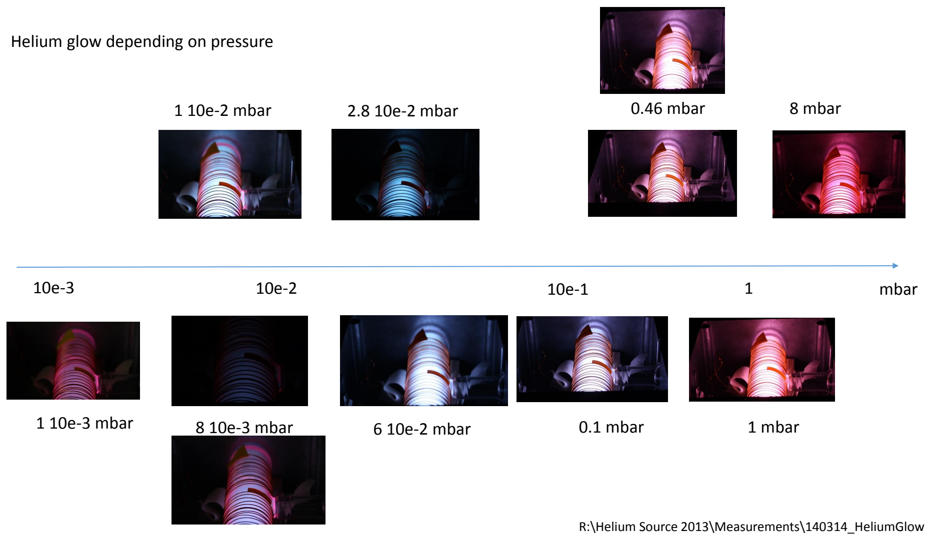

Figure 2.6: Helium glow as function of pressure. Image taken from project documentation.

3 Results

3.1 One skimmer

The initial setup only used one skimmer emplaced 8cm after the source. As can be seen in figure 3.1 there is no clear maximum of the intensity after 90cm at the MCP, instead the metastable atoms are spread out over the entire surface of the MCP.

In this experiment the source was moved perpendicular to the beam axis relative to the apparatus. One does not observe a change in the distribution of the metastable atoms as function of the position of the source. The integrated intensity over the entire screen however varies with the position of the source (Fig .3.2) to the top and to the right between the plate of the source and the mount. A Gaussian profile fit to the beam has a maximum at 10 mm in horizontal direction, and at 8 mm in vertical direction, with a spread of $\sigma = 13$ mm.

This behaviour can be explained that spread of the beam which is detected at the MCP is determined by the position of the skimmer and not the position of the source. A too large pressure difference between the atom beam and the chamber behind the skimmer causes a second expansion of the beam at the skimmer, determining the beam profile measured by the

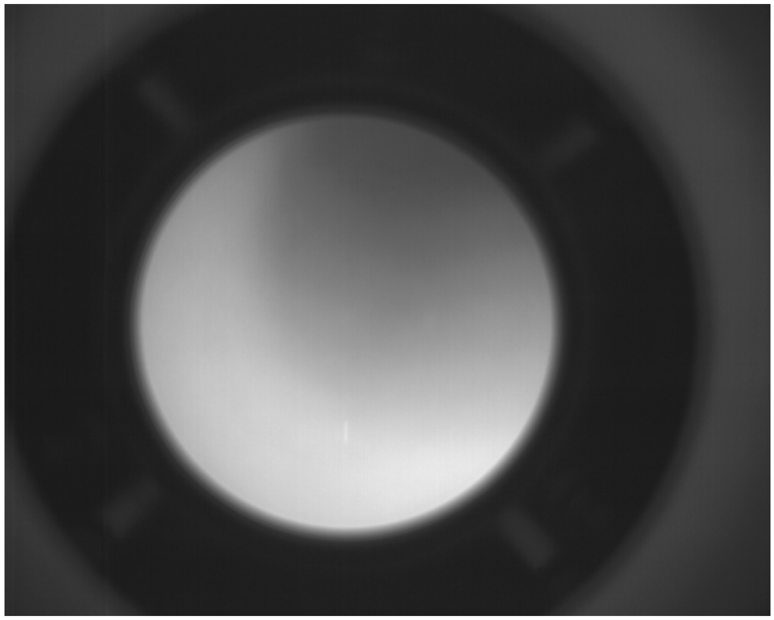

Figure 3.1: Image of the Beam. The atoms are spread over the entire disk of the phosphor screen. Features outside the disk are due to reflections from the chamber

MCP. This difference must be due to Eq. 1.1.4 larger than 10^{-1}mbar, using $\lambda_0 = d = 1$ mm, $T_0 = 300$ K, $a = 0.218$ nm [11]. The intensity of the beam is dependent on the intensity of the source at the skimmer, which is related to the position of the source.
This set of data (Fig. 3.2) allows the determination of the beam profile at the position of the nozzle, as the invariant beam shape allows the assumption that the fraction of atoms registered on the MCP from the total number of atoms passing through the nozzle is constant.
A spread of $13mm$ at the nozzle at a distance of $8cm$ gives a an angle of 9.3^o.

3.2 Two skimmers

The problem of the second expansion can be solved by the addition of a second skimmer in the zone of silence of the first skimmer. The resulting image (Figure 3.3) shows a clear beam compared to the previous image (Figure 3.1). Instead of spreading out over the entire screen, the beam is confined to a small area on the screen. A Gaussian fit to the beam profile

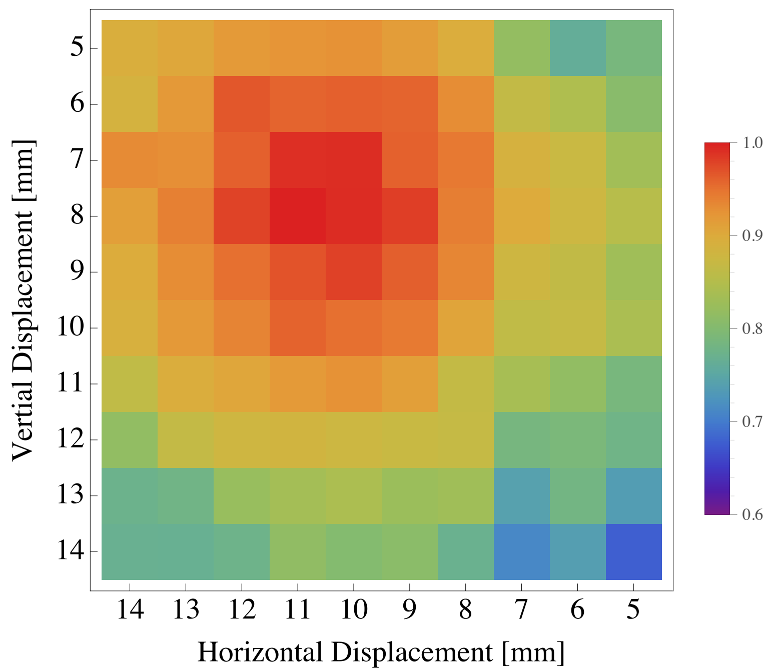

Figure 3.2: Integrated Intensity in arbitrary units as function of source position. The intensity falls off very slowly with respect to the position of the source.

gives a good fit with a width of $\sigma_H = 5.0mm$ horizontally and $\sigma_V = 4.6mm$ in the vertical. A crude geometric estimate for a beam passing two skimmers with $2mm$ respectively $1mm$ diameter spaced $8cm$ apart, shining on a screen $72cm$ away restricts the beam to a maximal circular area with a diameter $28mm$. This corresponds to an angle of divergence of $\approx 1^o$. The beam profile fits well in between those limits (Vertical lines in Fig. 3.4).

For the two skimmer setup the dependence of the intensity on the delay of the MCP was measured (Fig. 3.5). The delay triggers the voltage applied to the front plate of the MCP, increasing the potential difference, making it sensitive to incoming particles. In this experiment the duration of the HV pulse was $50\mu s$. By shifting the delay time the time axis was scanned. A Gaussian fit gives a maximum at $960\mu s$, with a width of $\sigma \approx 80\mu s$ for the signal from the metastable atoms. The first signal is due to light and ions that are created during the excitation process of the metastable atoms in the source.
From the delay measurement the velocity of the metastable atoms can be

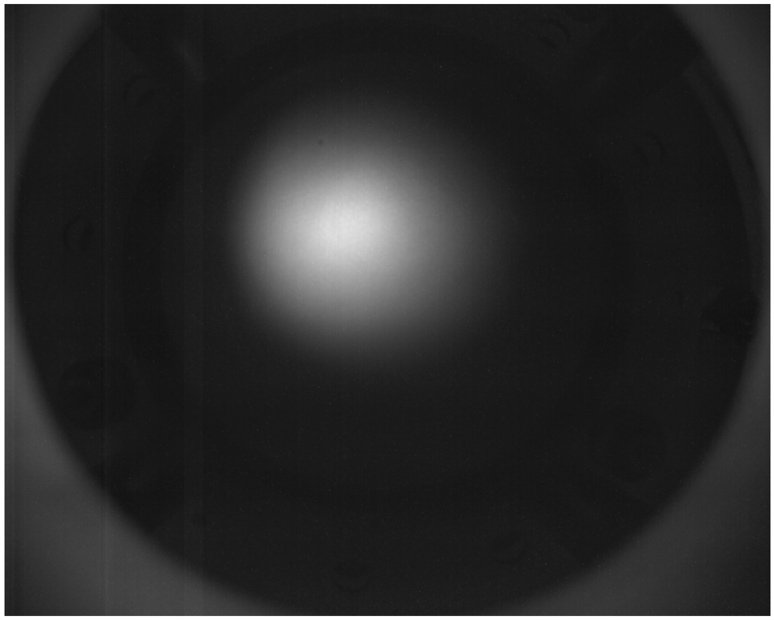

Figure 3.3: Image of the Beam. For this image two skimmers were employed, resulting in a much more focused beam than in Fig. 3.1.

calculated. With a distance of $90cm$ between source and MCP the atoms travel at a velocity of $2020/pm20\frac{m}{s}$ with a variance of $60\frac{m}{s}$. Taking the pulse duration into account this corresponds to a temperature of ≈ 12 K In transversal direction (Fig. 3.4) the variance can also be calculated, giving a variance of $40\frac{m}{s}$.

3.3 Spectroscopy

The spectrum of metastable He^* was recorded using the spectroscopy cell. Both the intensity of the probe beam in the Doppler-free saturation spectroscopy setup as well as the error signal generated by the Pound-Drever-Hall technique were recorded as function of the wavelength of the laser. The results (Fig.3.6) show three large, Doppler broadened resonances (1-1.5 GHz) with a central spike due to the saturation of He^* at zero velocity in beam direction corresponding to the three transitions $^3S_1 \to {}^3P_{2,1,0}$ in blue and the corresponding error signals in red.
We zoom into the transition which is used in the cooling process, $^3S_1 \to {}^3P_2$. One can see the saturated absorption peak in blue and the corresponding error signal in violet. The absorption peak is not a pure Lorenzian, but

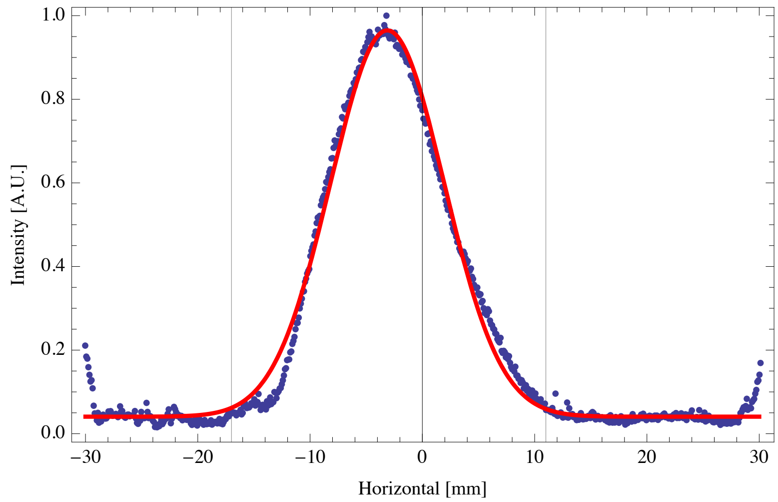

(a)

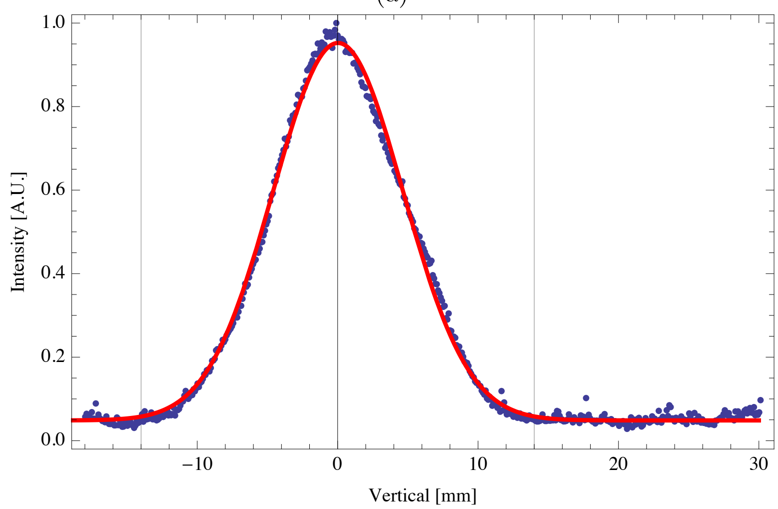

(b)

Figure 3.4: Cross section of the beam image. The vertical lines show the geometric restriction.

consists of 5 overlapping peaks. This is a result of dressing of the state due to the discharge AC frequency ($\approx$ 20 MHz) and the modulated sideband frequency, which are both greater than the natural linewidth of the state. The resulting peak has a width of $\approx$ 50 MHz.
The error signal has a zero crossing at the center of the saturation spike,

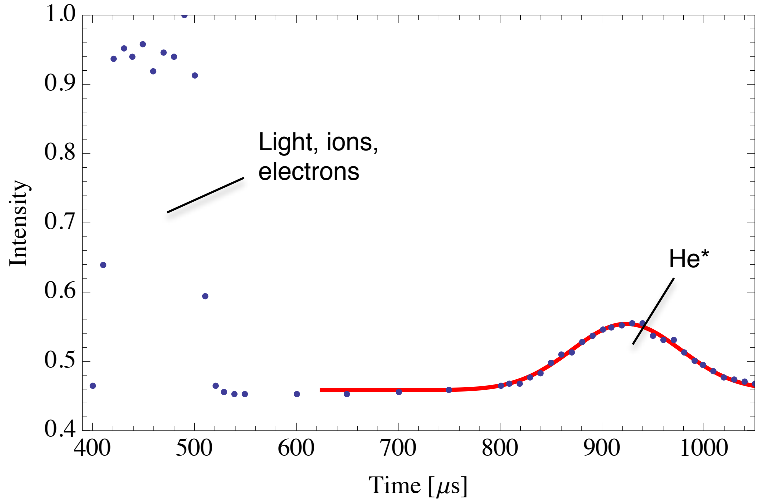

Figure 3.5: Integrated intensity as function of the delay of the MCP. The MCP was sensitive for a duration $50\mu s$. The delay time is the start time of the trigger pulse.

which is ideal for locking the laser frequency to.

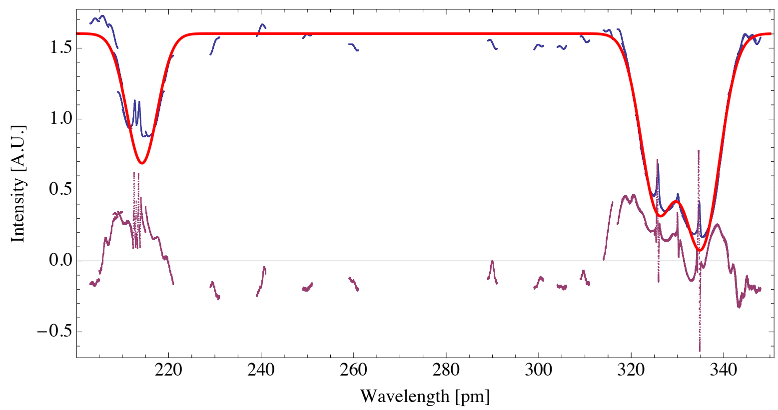

(a) Three resonances are visible in the spectrum.

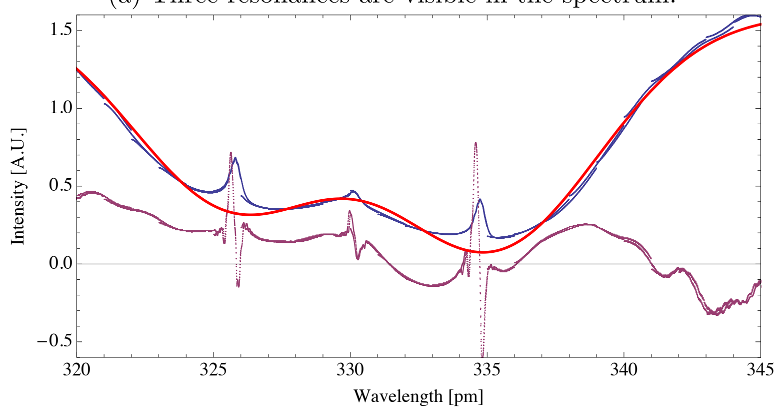

(b) At the center of the resonance an increase in transmission is observed.

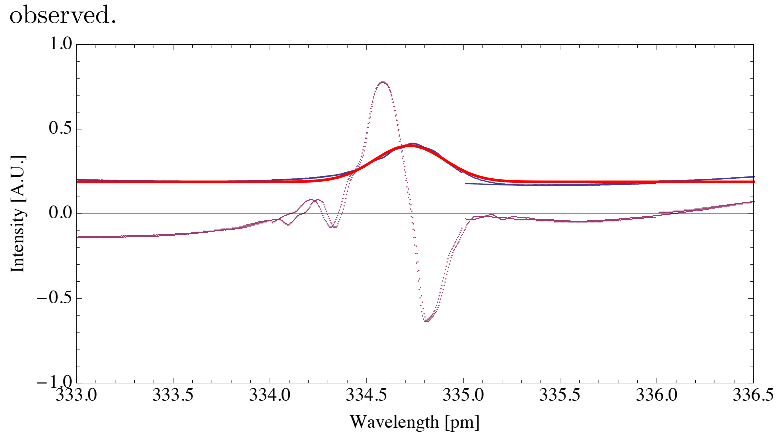

(c) The error signal has a zero crossing at the resonance.

Figure 3.6: Transmission spectrum of the spectroscopy with the corresponding error signal plotted both in arbitrary units. The laser is tuned to $1083.xxx\ nm$, where xxx denotes the x-axis.

4 Conclusion

The results show that the setup can successfully produce metastable He^* atoms, and with a MCP then detect and distinguish them from ions and light produced in the source. Using two skimmers, the angle of divergence can be reduced to $\approx 1^o$.
The spectroscopy setup shows the peak for the resonance at the transition from 2^3S_1 to the 2^3P_2 state, that are of interest for laser cooling.
During the writing of this work the spectroscopy setup was locked to the cooling laser to further reduce the divergence of the He^* beam, and the cooling setup has been currently being installed.

References

[1] Mateusz Kotyrba. Metastable-helium-4 source for cold atom experiments. Master's thesis, Universität Wien, 2010.

[2] Tobias Thiele. Towards a manipulation of trapped atoms in optical tweezers. Master's thesis, ETH Zürich, 2013.

[3] Robert S. Van Dyck, Charles E. Johnson, and Howard A. Shugart. Radiative lifetime of the 2^1s_0 metastable state of helium. *Phys. Rev. A*, 4:1327–1336, Oct 1971.

[4] D. J. Wineland, R. E. Drullinger, and F. L. Walls. Radiation-pressure cooling of bound resonant absorbers. *Phys. Rev. Lett.*, 40:1639–1642, Jun 1978.

[5] Harold J Metcalf and Peter Van der Straten. *Laser cooling and trapping.* Springer, 1999.

[6] Retrieved on 31. March 2014 from http://hyperphysics.phy-astr.gsu.edu/hbase/quantum/helium.html.

[7] D. W. Preston. Doppler-free saturated absorption: Laser spectroscopy. *American Journal of Physics*, 64:1432–1436, November 1996.

[8] R.W.P. Drever, J.L. Hall, F.V. Kowalski, J. Hough, G.M. Ford, A.J. Munley, and H. Ward. Laser phase and frequency stabilization using an optical resonator. *Applied Physics B*, 31(2):97–105, 1983.

[9] T. Halfmann, J Koensgen, and K Bergmann. A source for a high-intensity pulsed beam of metastable helium atoms. *Meas. Sci. Technol.*, 11:15101514, 2000.

[10] Mario Könz. Design, build-up and control of electronic equipment for the hybrid rydberg experiment. Master's thesis, ETH Zürich, 2014.

[11] ed. J. M. Lafferty. *Foundations of vacuum science and technology.* John Wiley & Sons, New York, 1998.

[12] Thomas F. Gallagher. *Rydberg Atoms.* Cambridge University Press, 1994.

[13] S. D. Hogan, J. A. Agner, F. Merkt, T. Thiele, S. Filipp, and A. Wallraff. Driving Rydberg-Rydberg transitions from a coplanar microwave waveguide. *Phys. Rev. Lett.*, 108:063004, Feb 2012.

[14] H. J. Metcalf and P. van der Straten. Laser cooling and trapping of atoms. *J. Opt. Soc. Am. B*, 20(5):887–908, May 2003.

[15] Sebastiaan Y. T. van de Meerakker, Hendrick L. Bethlem, and Gerard Meijer. Taming molecular beams. *Nat. Phys.*, 4(8):595–602, August 2008.

A LabView software

The LabView software is used to control and read out the camera monitoring the micro channel plate.

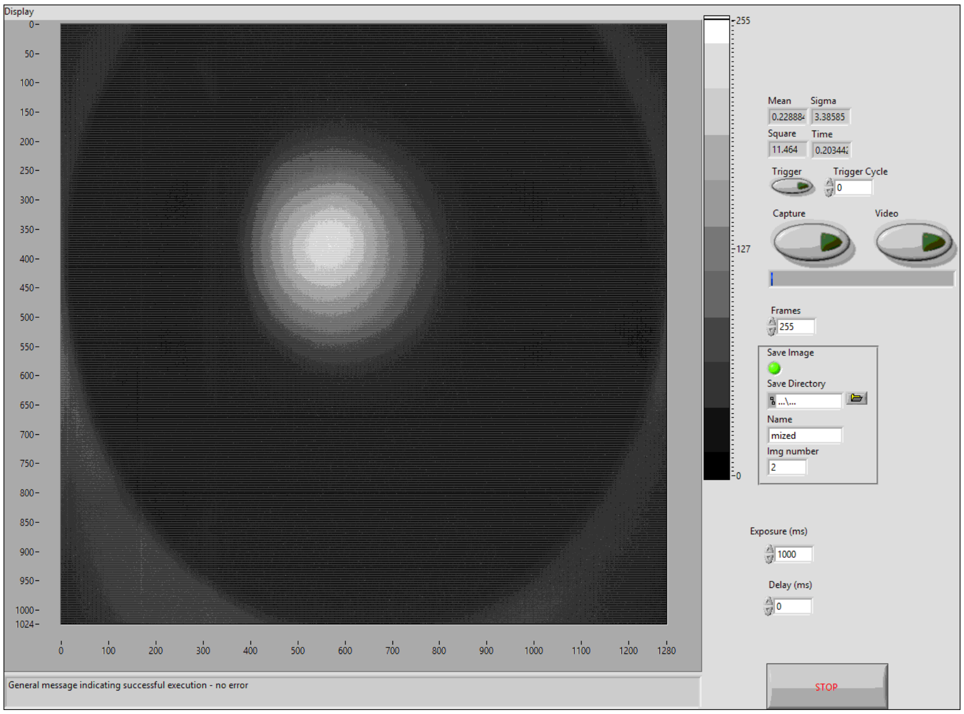

Figure A.1: Front end of the Labview software for controlling the camera

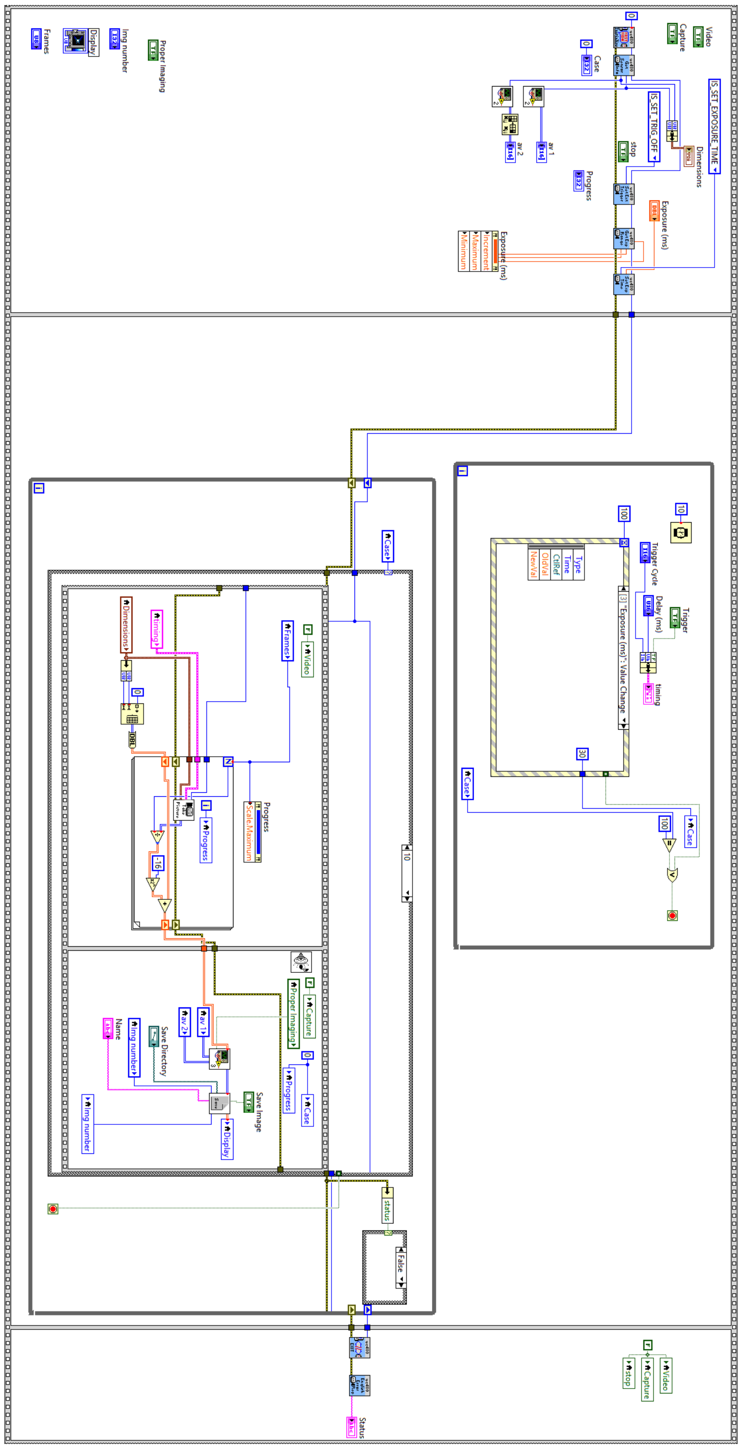

Figure A.2: Back end of the Labview software for controlling the camera

B MCP Voltage divider

The MCP voltage divider splits the voltage between front and back plate.

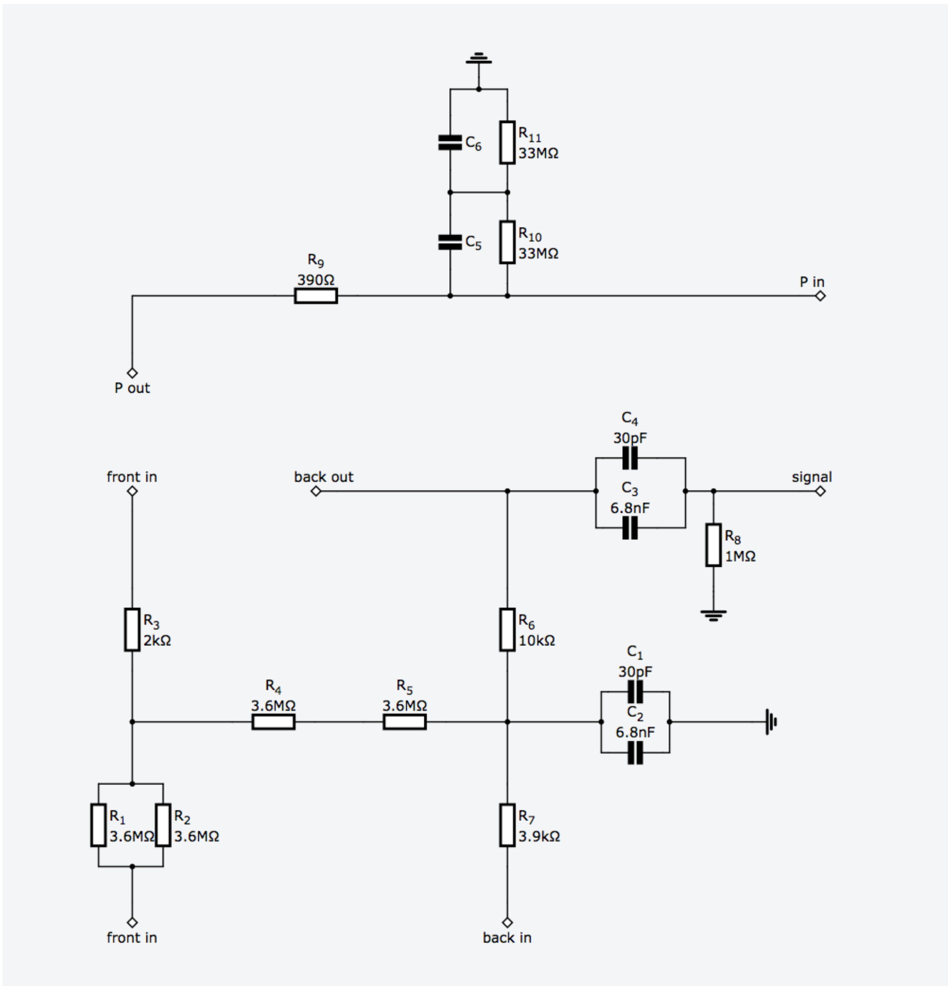

Figure B.1: Circuit diagram for voltage divider of the multi channel plate. $Front_{in}$, $Back_{in}$, P_{in} and $Signal$ lead to SHV connectors, while $Front_{out}$, $Back_{out}$ and P_{out} are connected to pins leading to the MCP.

C AC source

The AC source provides the necessary current for the filament heater.

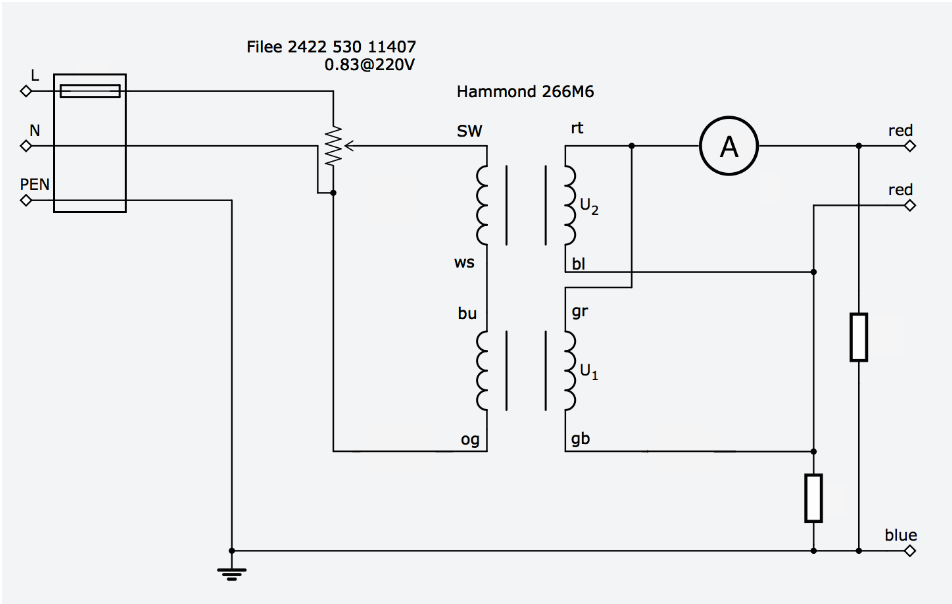

Figure C.1: Circuit diagram for the AC source.

ETH

Eidgenössische Technische Hochschule Zürich
Swiss Federal Institute of Technology Zurich

Declaration of originality

The signed declaration of originality is a component of every semester paper, Bachelor's thesis, Master's thesis and any other degree paper undertaken during the course of studies, including the respective electronic versions.

Lecturers may also require a declaration of originality for other written papers compiled for their courses.

I hereby confirm that I am the sole author of the written work here enclosed and that I have compiled it in my own words. Parts excepted are corrections of form and content by the supervisor.

Title of work (in block letters):

Metastable Helium Source

Authored by (in block letters):

For papers written by groups the names of all authors are required.

Name(s):	First name(s):
Gerster	Lukas

With my signature I confirm that

- I have committed none of the forms of plagiarism described in the 'Citation etiquette' information sheet.
- I have documented all methods, data and processes truthfully.
- I have not manipulated any data.
- I have mentioned all persons who were significant facilitators of the work.

I am aware that the work may be screened electronically for plagiarism.

Place, date

Zürich 29 July 2014

Signature(s)

For papers written by groups the names of all authors are required. Their signatures collectively guarantee the entire content of the written paper.